

Image-guided 3D interpolation of borehole data

Dave Hale, Center for Wave Phenomena, Colorado School of Mines

SUMMARY

A blended neighbor method for image-guided interpolation enables resampling of borehole data onto a uniform 3D sampling grid, without picking horizons. Borehole measurements gridded in this way become new 3D images of subsurface properties. Property values conform to geologic layers and faults apparent in the seismic image that guides the interpolation.

INTRODUCTION

Seismic images are often used to guide the interpolation of subsurface properties that are measured more directly and (usually) more precisely in boreholes. Figure 1 provides an example for a 3D seismic image and sonic (P-wave velocity) logs from the Teapot Dome oilfield in Wyoming. These data are provided by the Rocky Mountain Oilfield Test Center, a facility of the U.S. Department of Energy (Anderson, 2009). Figure 1b shows interpolated velocities, displayed with translucent color so that the corresponding three slices of the 3D seismic image are visible as well. At depths where sonic logs are available, the interpolation of velocities is guided by the seismic image.

In a more conventional seismic interpretation, we might first pick horizons corresponding to coherent reflections in the seismic image. Two examples are shown in Figure 1c and d. These two horizons correspond to the Crow Mountain and Tensleep formations, and are provided as part of the Teapot Dome data set. Typically, we would pick horizons like these interactively, with or without help from automatic event-tracking software. One reason we might construct horizon surfaces like these is to facilitate interpolation of properties measured in boreholes.

I interpolated the velocities shown in Figure 1 without using horizons. Instead, I used the seismic image to automatically and more directly guide 3D interpolation of the velocity logs. Although the horizons in Figure 1c and d were not used, they coincide with low-velocity layers apparent in the 3D interpolation shown in Figure 1b.

IMAGE-GUIDED INTERPOLATION

Let us assume that spatially scattered data to be interpolated are a set

$$\mathcal{F} = \{f_1, f_2, \dots, f_K\} \quad (1)$$

of K known sample values $f_k \in \mathbb{R}$ that correspond to a set

$$\mathcal{X} = \{\mathbf{x}_1, \mathbf{x}_2, \dots, \mathbf{x}_K\} \quad (2)$$

of K known sample points $\mathbf{x}_k \in \mathbb{R}^n$. The known samples (f_k, \mathbf{x}_k) may be scattered such that the n -dimensional sample points \mathbf{x}_k in the set \mathcal{X} may have no regular geometric structure. The classic interpolation problem is to use the known samples to construct a function $q(\mathbf{x}) : \mathbb{R}^n \rightarrow \mathbb{R}$, such that $q(\mathbf{x}_k) = f_k$.

As stated, this problem has no unique solution; there exist an infinite number of functions $q(\mathbf{x})$ that satisfy the interpolation conditions $q(\mathbf{x}_k) = f_k$. Additional criteria may include measures of smoothness, robustness, and efficiency. Because tradeoffs exist among such criteria, a variety of methods for interpolating scattered data are commonly used today.

In this paper I add the requirement that the interpolation should conform to features in a uniformly sampled image, as in Figure 1. That is, the interpolation must be *image-guided*.

Blended neighbor interpolation

The blended neighbor method (Hale, 2009) was developed to facilitate image-guided interpolation. This process consists of two steps:

Step 1: solve the eikonal equation

$$\begin{aligned} \nabla t(\mathbf{x}) \cdot \mathbf{D}(\mathbf{x}) \nabla t(\mathbf{x}) &= 1, & \mathbf{x} \notin \mathcal{X}; \\ t(\mathbf{x}_k) &= 0, & \mathbf{x}_k \in \mathcal{X} \end{aligned} \quad (3)$$

for

$t(\mathbf{x})$: the minimal time from \mathbf{x} to the nearest known sample point \mathbf{x}_k , and

$p(\mathbf{x})$: the value f_k corresponding to the sample point \mathbf{x}_k nearest to the point \mathbf{x} .

Step 2: solve the blending equation

$$q(\mathbf{x}) - \frac{1}{2} \nabla \cdot \mathbf{t}^2(\mathbf{x}) \mathbf{D}(\mathbf{x}) \nabla q(\mathbf{x}) = p(\mathbf{x}), \quad (4)$$

for the blended neighbor interpolant $q(\mathbf{x})$.

Here, *time* is simply a short word for *non-Euclidean distance*. By this measure of distance, a sample point \mathbf{x}_k is *nearest* to a point \mathbf{x} if the time $t(\mathbf{x})$ along some path to \mathbf{x}_k is less than that for any other sample point. In step (1), I compute this minimal-time map $t(\mathbf{x})$ by solving the eikonal equation 3.

The metric tensor field $\mathbf{D}(\mathbf{x})$ provides the anisotropic and spatially varying coefficients of that eikonal equation. Intuitively, we must choose the tensor field $\mathbf{D}(\mathbf{x})$ so that, by our time measure of non-Euclidean distance, two points within the same geologic formation are near, while two points in different formations are much farther away. In this way, known sample values f_k for sample points \mathbf{x}_k that are geologically nearby are given the most weight in any interpolated value $q(\mathbf{x})$.

In step (1), as I compute the time $t(\mathbf{x})$ from each point \mathbf{x} to the location \mathbf{x}_k of the nearest known sample, I also record the value $p(\mathbf{x}) = f_k$ of that nearest known sample. The function $p(\mathbf{x})$ is therefore a *nearest neighbor* interpolant.

In step (2), I compute the *blended neighbor* interpolant $q(\mathbf{x})$

Image-guided 3D interpolation

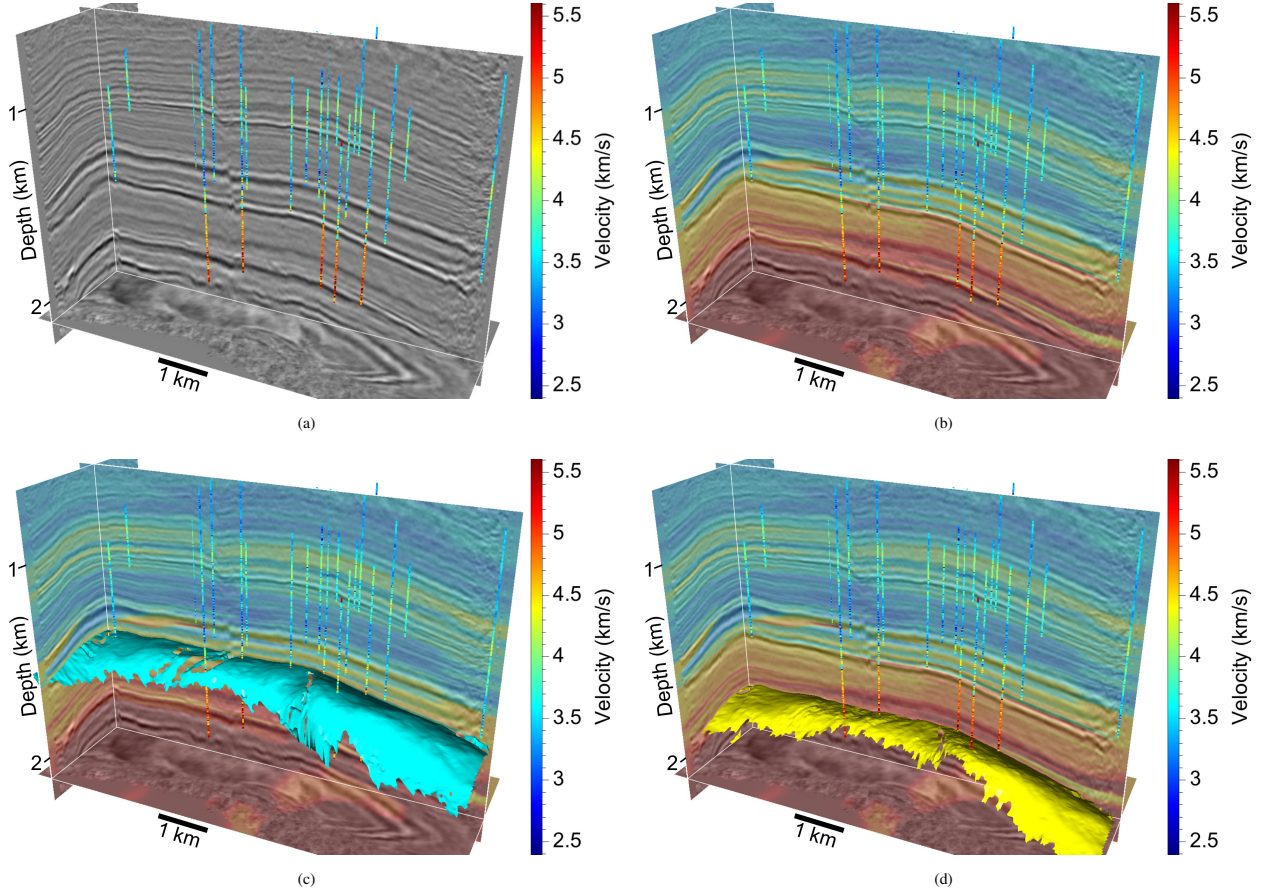


Figure 1: Slices of a 3D seismic image (a) with P-wave velocities measured in boreholes and an image-guided 3D interpolation (b) of those measured velocities. Two low-velocity layers in the 3D interpolated velocity image conform to the Crow Mountain (c) and Tensleep (d) horizons that were picked interactively (by others) from the 3D seismic image. Only the seismic image, not the horizons, was used to guide the 3D interpolation of the velocity logs.

by smoothing the nearest neighbor interpolant $p(\mathbf{x})$; and the extent of smoothing is controlled by the time map $t(\mathbf{x})$. At any known sample point \mathbf{x}_k , equation 3 states that $t(\mathbf{x}_k) = 0$, so that no smoothing is performed, and equation 4 becomes simply $q(\mathbf{x}_k) = p(\mathbf{x}_k) = f_k$. In other words, the function $q(\mathbf{x})$ interpolates exactly the known sample values.

TEAPOT DOME EXAMPLE

The freely available Teapot Dome data set, which includes a time-migrated 3D seismic image and hundreds of well logs (Anderson, 2009), enables a realistic demonstration of image-guided 3D interpolation of borehole data. For this purpose, I selected four types of well logs: P-wave velocity, density, porosity and gamma ray.

For each type of log I obtained the set of known samples (f_k, \mathbf{x}_k) with a simple binning and averaging procedure. First, I rounded the spatial coordinates of each well log sample to the coordinates of the nearest bin in the interpolation grid. Each known sample location \mathbf{x}_k therefore corresponds to one such bin, and

each known sample value f_k is the average of all well log samples for which \mathbf{x}_k is the nearest bin. After this binning and averaging procedure, only those bins in the interpolation grid that are intersected by well logs of the appropriate type have values. Values for other bins in the grid are unknown and will be interpolated using the two-step process of equations 3 and 4.

Before solving equations 3 and 4, we must first specify a metric tensor field $\mathbf{D}(\mathbf{x})$. I derived $\mathbf{D}(\mathbf{x})$ from structure tensors (van Vliet and Verbeek, 1995; Fehmers and Höcker, 2003) computed from the seismic image.

Nearest neighbor interpolation

The known samples (f_k, \mathbf{x}_k) obtained by initial gridding of well log data and the tensor field $\mathbf{D}(\mathbf{x})$ computed from the image are the parameters required for step (1) of image-guided interpolation. In this step I simultaneously compute both the time map $t(\mathbf{x})$ and the nearest neighbor interpolant $p(\mathbf{x})$ by solving a finite-difference approximation of the eikonal equation 3.

Figure 2 displays the nearest neighbor interpolants $p(\mathbf{x})$ for

Image-guided 3D interpolation

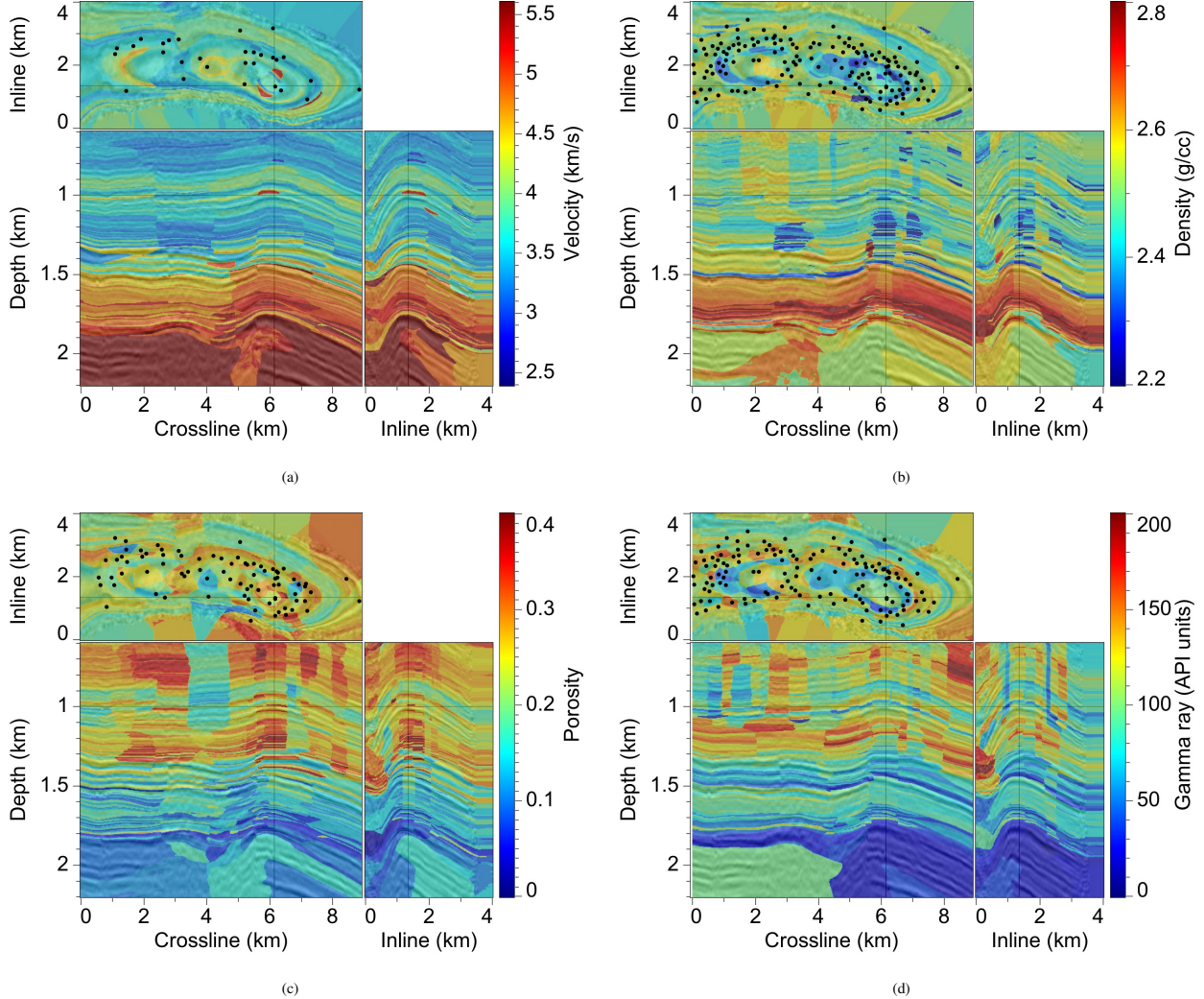


Figure 2: Image-guided nearest neighbor interpolation of velocity (a), density (b), porosity (c) and gamma ray (d) logs.

four different borehole measurements. Again, interpolated values are displayed with translucent color on top of the seismic image used to guide the interpolation.

For each log type, black dots in the horizontal constant-depth slices indicate the intersections of well logs with these slices. These dots represent only a tiny subset of the many well log samples (above and below these slices) used to perform the 3D interpolation.

As expected, all of the nearest neighbor interpolants shown in Figure 2 exhibit discontinuities. I chose the slices displayed in Figure 2 specifically to highlight some of those discontinuities. Most of these discontinuities do not coincide with geologic faults. Rather, they reflect inconsistencies among properties measured within wells and those measured within their nearest neighbor wells.

For example, anomalously low (light blue) porosities are apparent in the upper middle part of the vertical crossline slice in

Figure 2c. Image-guided nearest neighbor interpolation may lead us to look more closely at the porosity logs of nearby wells, to look for possible sources of error.

At depths greater than 1.9 km, large areas of constant interpolated values are apparent in Figures 2. Because no wells extend to these depths, all of the well log samples that lie in shallower geologic layers appear to be relatively far away, so that the nearest neighbor sample value is a poor interpolant.

Blended neighbor interpolation

Step (2) of image-guided interpolation is the solution of a finite-difference approximation of the blending equation 4. Parameters in this equation include the metric tensor field $\mathbf{D}(\mathbf{x})$, as well as the time map $t(\mathbf{x})$ and nearest neighbor interpolant $p(\mathbf{x})$. Figure 3 shows slices of blended neighbor interpolants $q(\mathbf{x})$ corresponding to the nearest neighbor interpolants $p(\mathbf{x})$ shown in Figure 2.

The blended neighbor interpolants shown in Figure 3 are con-

Image-guided 3D interpolation

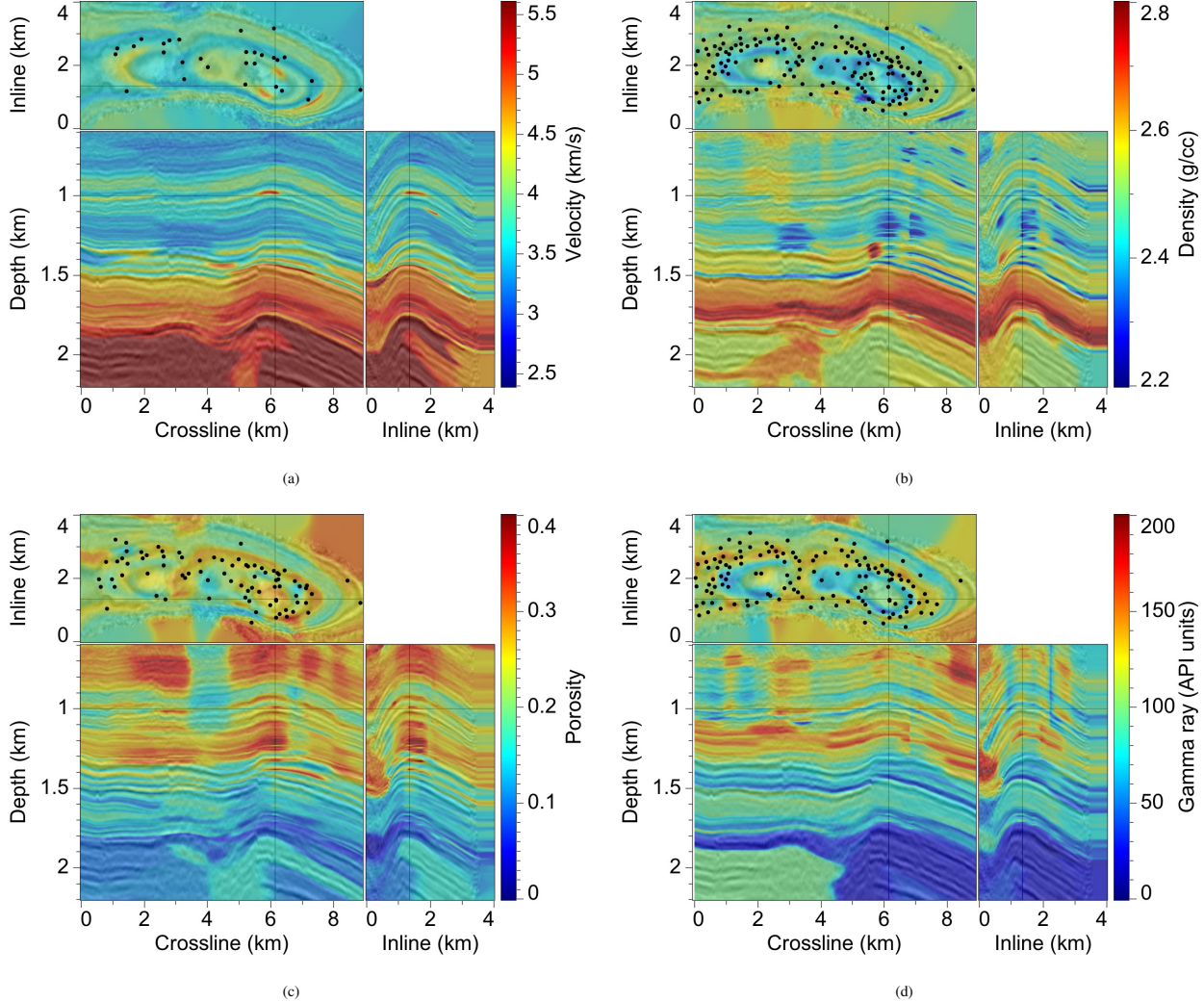


Figure 3: Image-guided blended neighbor interpolation of velocity (a), density (b), porosity (c) and gamma ray (d) logs.

sistent with the borehole data and structures apparent in the seismic image. For example, the strong reflector at a depth of about 1.5 km coincides with a significant change in both velocity and density, the factors of acoustic impedance. A thin layer at that depth with relatively low velocity, low density, high porosity, and low gamma ray radioactivity corresponds to the Crow Mountain sandstone formation marked by the light-blue horizon displayed in Figure 1c. The low (dark blue) density of this formation is especially visible in the slices of interpolated densities.

CONCLUSION

In practice both the nearest neighbor and blended neighbor image-guided interpolants may be useful. The nearest neighbor interpolant may be used to detect inconsistencies in borehole data acquired within a single seismically imaged geologic layer. Well log sample values that are inconsistent with those

of geologically nearby log samples may be erroneous and perhaps should be discarded.

The nearest neighbor interpolant is also a necessary first step toward computing the smoother blended neighbor interpolant. Within seismically imaged layers, the blended neighbor interpolant is continuous and therefore geologically more reasonable than the discontinuous nearest neighbor interpolant.

ACKNOWLEDGMENTS

Thanks to the Rocky Mountain Oilfield Test Center, a facility of the U.S. Department of Energy, for providing the 3D seismic image, horizons, and well logs used in this study. Thanks also to Transform Software and Services, especially Amelia Webster, for providing their time-to-depth conversion of the 3D seismic image. I also thank Chris Engelsma for explaining to me the uses and significance of various types of well logs.

Image-guided 3D interpolation

REFERENCES

- Anderson, T., 2009, History of geologic investigations and oil operations at Teapot Dome, Wyoming: Presented at the 2009 AAPG Annual Convention.
- Fehmert, G., and C. Höcker, 2003, Fast structural interpretation with structure-oriented filtering: *Geophysics*, **68**, 1286–1293.
- Hale, D., 2009, Image-guided blended neighbor interpolation of scattered data: 79th Annual International Meeting, SEG, Expanded Abstracts, 1127–1131.
- van Vliet, L., and P. Verbeek, 1995, Estimators for orientation and anisotropy in digitized images: Proceedings of the first annual conference of the Advanced School for Computing and Imaging, 442–450.